

The Relative Contributions of Polymer Annealing and Subunit Exchange to Microtubule Dynamics in Vitro

Stephen W. Rothwell, William A. Grasser, Howard N. Baker, and Douglas B. Murphy

Department of Cell Biology and Anatomy, The Johns Hopkins University School of Medicine, Baltimore, Maryland 21205

Abstract. Microtubules that are free of microtubule-associated protein undergo dynamic changes at steady state, becoming longer but fewer in number with time through a process which was previously assumed to be based entirely on mechanisms of subunit exchange at polymer ends. However, we recently demonstrated that brain and erythrocyte microtubules are capable of joining end-to-end and suggested that polymer annealing may also affect the dynamic behavior of microtubules in vitro (Rothwell, S. W., W. A. Grasser, and D. B. Murphy, 1986, *J. Cell Biol.* 102:619-627). In the present study, we first show that annealing is a general property of cytoplasmic microtubules and is not a

specialized characteristic of erythrocyte microtubules by documenting annealing between tyrosinolated and detyrosinolated brain microtubules. We then examine the contributions of polymer annealing and subunit exchange to microtubule dynamics by analyzing the composition and length of individual polymers in a mixture of brain and erythrocyte microtubules by immunoelectron microscopy. In concentrated preparations of short-length microtubules at polymer-mass steady state, annealing was observed to be the principal factor responsible for the increase in polymer length, whereas annealing and subunit exchange contributed about equally to the reduction in microtubule number.

MICROTUBULES that are free of microtubule-associated protein (MAP)¹ exhibit dynamic behavior at steady state in vitro, becoming fewer in number but longer in length with time (8, 20, 21, 29, 39). Mitchison and Kirschner, who were the first to describe the phenomenon in detail, called the process "dynamic instability" and postulated that it was due to a mechanism of subunit exchange at the ends of microtubules and was related to the differential stability of microtubules terminating in either GTP- or GDP-tubulin (13, 28, 29). The theory was based on experimental evidence gathered over several years by Carlier and co-workers regarding the relationship of the rates of microtubule assembly and disassembly to the rate of GTP hydrolysis (5-7, 14, 15). In essence, the dynamic instability theory holds that microtubules composed of GDP-tubulin cores are inherently unstable, and that upon loss of stabilizing GTP-tubulin caps, polymers can depolymerize and disappear. The subunits released from these microtubules would exchange GDP for GTP and would then be free to reassociate with the ends of the remaining microtubules. In this way, the observed decrease in microtubule number and increase in polymer length could be explained solely by a mechanism of subunit exchange. However, we recently demonstrated that microtubule polymers can join end-to-end, and that depending on the conditions, as much as 50% of the microtubule population anneals within 1 min. These observations suggested that polymer annealing could also affect the dy-

amic behavior of microtubules in vitro (39). However, the conditions under which annealing occurred and its relative importance compared with subunit exchange in determining microtubule dynamics were not understood.

One question deriving from our previous work on annealing between brain and erythrocyte microtubules was whether all microtubules could anneal. Inasmuch as erythrocyte tubulin is known to contain its own unique assembly properties and biochemical characteristics (31, 32), it could be argued that the annealing we observed was due to the presence of this particular tubulin variant. To determine whether annealing was a property of microtubules in general, we prepared microtubules from tyrosinolated and detyrosinolated brain tubulin and employed an antibody specific for the tyrosinolated form of α -tubulin in an immunoelectron microscopic assay to discriminate between the two "homologous" tubulin types (19, 47). Previous studies by Raybin and Flavin (36) and Kumar and Flavin (22) demonstrated that tyrosinolated and detyrosinolated tubulin polymerize equally well in vitro, implying that the in vitro assembly properties are not significantly different. Therefore, we used this system to examine the rate and extent of annealing between homologous brain microtubules.

To study further the process of polymer annealing and determine its specific contribution to microtubule dynamics, we examined individual polymers in mixtures of brain and erythrocyte microtubules by immunogold microscopy that used an antiserum specific for the β -subunit of erythrocyte tubulin. The patterns and densities of immunogold labeling

1. *Abbreviations used in this paper:* MAP, microtubule-associated protein; PC, phosphocellulose.

allowed us to distinguish erythrocyte and brain tubulin domains in heteropolymers as well as copolymers that contained a mixture of both tubulin subunits. By measuring the number and length of the different tubulin domains and the arrangement of domains within polymers, we were able to calculate the relative contributions of polymer annealing and subunit exchange to microtubule dynamics. In concentrated preparations of short microtubules prepared by extensive shearing, annealing was observed to be a major factor in determining changes in polymer length and number at steady state.

Materials and Methods

Preparation of Chicken Brain and Erythrocyte Tubulin

Chicken brain tubulin was isolated by the method of Dentler et al. (9) in 0.1 M Pipes buffer containing 1 mM MgCl₂, 2 mM EGTA, 1 mM GTP, and 4 M glycerol.

Chicken erythrocyte tubulin was prepared from chicken blood by the method of Murphy and Wallis (32). Tubulin was purified free of MAPs by ion-exchange chromatography using Whatman P-11 phosphocellulose (PC) (Whatman, Inc., Clifton, NJ) (37) and processed through a cycle of microtubule assembly and disassembly once before use to remove any inactive subunits. Unless stated otherwise, microtubule assembly buffer was 0.1 M Na-Pipes at pH 6.94 containing 1 mM MgCl₂ and 1 mM GTP and supplemented with 5% glycerol.

Preparation of Microtubules Used to Study Microtubule Dynamics

Purified tubulin was concentrated by polymerizing either erythrocyte or brain PC tubulin in 0.1 M Pipes, pH 6.94, containing 10 mM MgCl₂, 1 mM GTP, and 20% glycerol, sedimenting, and resuspending at 5–8 mg/ml in assembly buffer containing 1 mM MgCl₂ and 5% glycerol as defined above. After polymerization, the microtubules were sheared by 10 passes through a 27-gauge needle (18) to prepare microtubules with a mean length of 1–2 μ m. These short microtubules comprised the starting material used for studying annealing.

Preparation of Detyrosinated Brain Microtubules

Detyrosinated brain microtubules were prepared by polymerizing brain microtubule protein at 10 mg/ml in assembly buffer containing 0.15 μ g/ml carboxypeptidase A at 37°C for 30 min (1, 34). 1,10-phenanthroline (11) was added to 50 μ M, and the microtubules were pelleted at 40,000 *g* for 40 min at 30°C. The pellet was resuspended in 25 mM Pipes and passed over a 3-ml PC bed equilibrated in 25 mM Pipes. The protein peak was pooled and the constituents of assembly buffer were restored to their original concentrations using concentrated stock solutions of Pipes, MgCl₂, GTP, and glycerol. The protein solution was centrifuged at 150,000 *g* for 30 min at 5°C, the supernatant then was polymerized at 37°C for 40 min, and the resulting microtubules were sheared as described above. Noncarboxypeptidase-treated tubulin was processed in parallel in the same way. For taxol-stabilized microtubules, taxol was added to 10 μ M and the protein was repolymerized and sheared to produce the material for annealing experiments. Their lengths were comparable to nontaxol-treated microtubules.

Conditions for Microtubule Annealing

Annealing was initiated by mixing together different kinds of microtubule polymers. In the case of brain–brain microtubule annealing, detyrosinated brain microtubules were mixed with tyrosinated brain microtubules in a 1:1 ratio immediately after shearing and incubated for 60 min at 37°C. For erythrocyte–brain microtubule annealing, the time between shearing and mixing ranged 0–10 min. For all experiments aliquots of the incubation mixtures were diluted to 0.1–0.2 mg/ml at various times in assembly buffer containing 1% glutaraldehyde and prepared for EM.

Procedures for Immunoelectron Microscopy

EM grids containing glutaraldehyde-fixed microtubules were stained according to the method of Rothwell et al. (38) using rabbit polyclonal anti-

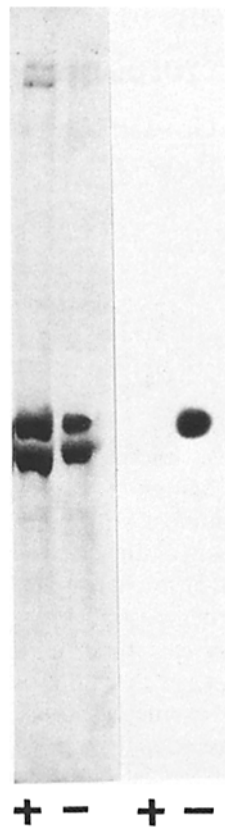


Figure 1. Demonstration of the specificity of an antibody to tyrosinated α -tubulin by immunoblotting. Chicken brain microtubule protein was fractionated by electrophoresis on a 10% gel, pH 9.1 (32) and transferred to nitrocellulose paper (45). The paper was incubated successively in solutions containing antibody specific for tyrosinated tubulin (diluted 1:1,000), rabbit anti-rat immunoglobulin antibody (5 μ g/ml), and ¹²⁵I-protein A. The left panel shows Amido black staining patterns of carboxypeptidase A-treated (+) or untreated (-) microtubule protein. The right panel shows the corresponding autoradiogram.

bodies specific for the β -subunit of chicken erythrocyte tubulin (25 μ g/ml) or 1,000-fold dilutions of a rat monoclonal antibody specific for tyrosinated α -subunit of brain tubulin developed by Kilmartin et al. (19, 47). For EM we used protein A-gold (43) to detect the sites of antibody labeling. In the case of brain microtubules labeled with rat monoclonal antibodies we used affinity-purified rabbit anti-rat immunoglobulin antibody (Boehringer Mannheim Biochemicals, Indianapolis, IN) at 10 μ g/ml for 30 min as an intermediate step to obtain adequate labeling.

Measurements of the lengths of decorated microtubules were made using a Zeiss EM 10A electron microscope (Carl Zeiss, Inc., Thornwood, NY). All measurements were normalized by measuring a constant total length (constant polymer mass) of \sim 750 μ m of polymer (\sim 200 microtubules and 600 distinct domains) for each time point of the two experimental conditions. Because increasing the sample size from 325 to 750 μ m in total length did not significantly change the mean and standard deviation of microtubule length in case B, 0 min (3.9 ± 2.3 and 3.6 ± 1.9 μ m, respectively), we felt confident that 750 μ m in total length reliably defined the sample.

Determination of Protein Concentration

Total protein concentrations were determined by the Bradford protein assay (3). Bovine serum albumin (BSA) was used as a standard.

Biochemical Materials

Pipes, sodium salt, was obtained from Calbiochem-Behring Corp. (La Jolla, CA). Other chemicals and nucleotides were obtained from Sigma Chemical Co. (St. Louis, MO).

Results

Annealing between Tyrosinated and Detyrosinated Chicken Brain Microtubules

To determine whether polymer annealing was a general property of cytoplasmic microtubules, we examined annealing between tyrosinated and detyrosinated chicken brain

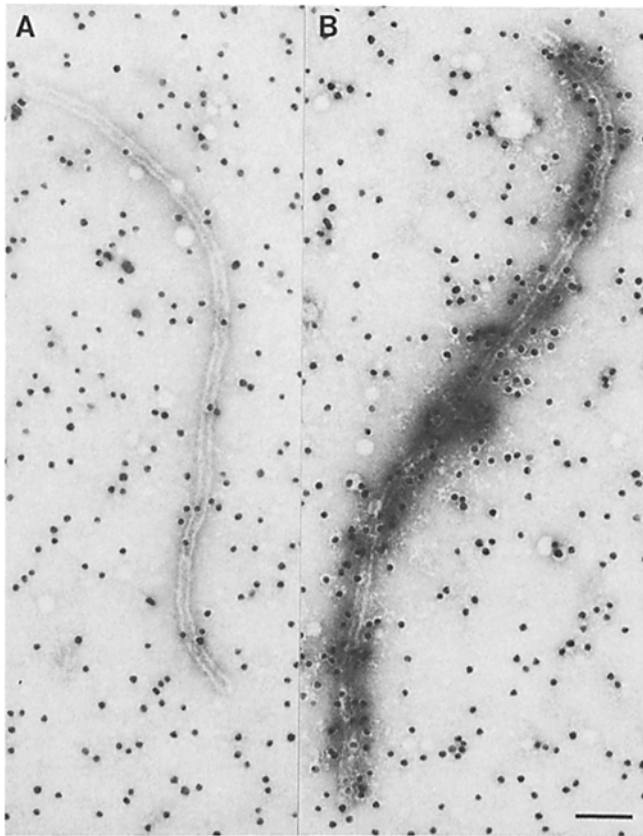


Figure 2. Microtubules labeled by tyrosinated tubulin antibody. Microtubules were polymerized from chicken brain PC-tubulin (5.2 mg/ml) which was either treated (A) or not treated (B) with carboxypeptidase A (0.2 U/ml). The two types of polymers were fixed in 1% glutaraldehyde in assembly buffer and incubated with tyrosinated tubulin antibody (diluted 1:1,000), rabbit anti-rat IgG antibody (10 μ g/ml) and protein A-gold. Bar, 0.1 μ m.

microtubules by immunoelectron microscopy after labeling with a monoclonal antibody specific for tyrosinated α -tubulin. The specificity of the antibody for the tyrosinated form of chicken brain tubulin is shown by immunoblotting in Fig. 1 and by immunoelectron microscopy in Fig. 2. Microtubules assembled from detyrosinated tubulin (Fig. 2 A) were unlabeled, whereas the tyrosinated microtubules (Fig. 2 B) were clearly labeled.

Preparations of tyrosinated and detyrosinated brain microtubules at 5 mg/ml were sheared and immediately mixed at 37°C. At various times after mixing, aliquots were fixed with glutaraldehyde. The microtubules were then labeled with mouse anti-tubulin and goat anti-mouse antibodies and protein A-gold before examination by electron microscopy. The conditions under which microtubule dynamics were observed were similar to those seen in a previous study (39): (a) the system was at polymer mass steady state; (b) microtubule number decreased while length increased; (c) the mean lengths of the different types of tubulin domains within annealed and elongated microtubules were conserved over a time course lasting several hours. Fig. 3, A and B show examples of annealed brain microtubules. The pattern of labeling using the two antibodies described above is less distinct than that obtained for erythrocyte microtubules using a single antibody, (compare Fig. 3 with Fig. 4),

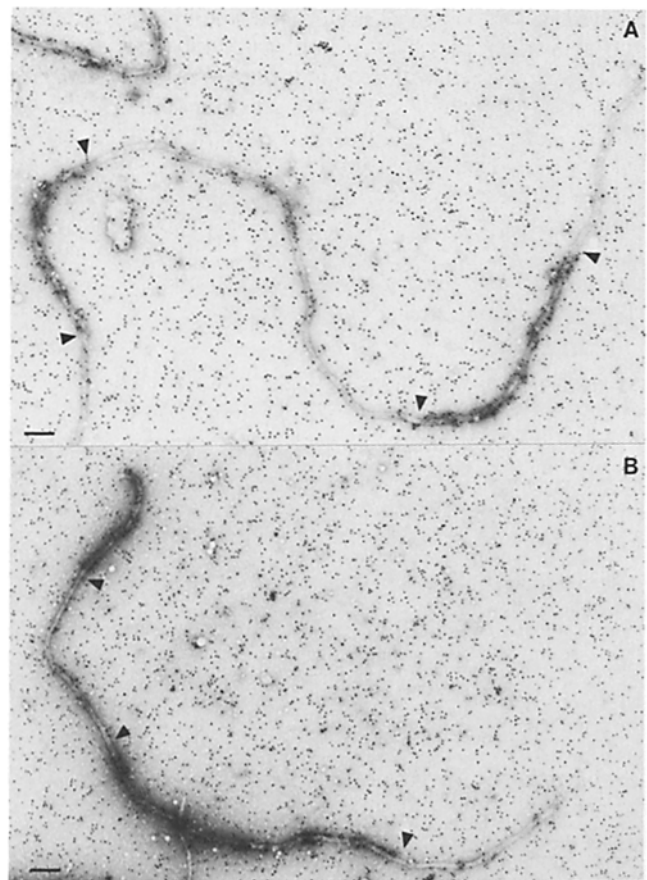


Figure 3. Annealing of brain microtubules. Microtubules polymerized from brain tubulin pretreated with carboxypeptidase A were mixed with untreated microtubules. After 20 min incubation at 37°C, the samples were fixed in 1% glutaraldehyde in assembly buffer and prepared for EM as described. Arrowheads indicate transitions from one tubulin type to another. Bar, 0.2 μ m.

but was adequate to document homologous brain microtubule annealing and calculate initial annealing rates. At \sim 10 s, few annealed microtubules were observed (2% of the total microtubule population), but by 10 min 20% of the microtubules were annealed, with the frequency increasing to 49% after 20 min (Table I c). The initial rate of annealing between brain microtubules was 10–20-fold lower than the previously observed rate between erythrocyte and brain microtubules (Table I e). Although the initial rate was lower than for erythrocyte–brain microtubule annealing, the extent of polymer annealing after 1 h was similar in both cases. In part, the difference in initial rates may be due to the lower concentration of microtubule ends in the experiment involving homologous brain microtubules. However, as discussed below, we believe that erythrocyte microtubules anneal at a greater rate than brain microtubules.

To establish whether the increased rate of annealing of erythrocyte and brain microtubules was due to differences in stability and equilibrium properties of the erythrocyte tubulin polymer, we also examined annealing of tyrosinated and detyrosinated microtubules in the presence of 10 μ M taxol. In contrast to previous observations (39), not much difference was observed in the initial rate of annealing in the two samples (Table I c and d, vs. e and f).

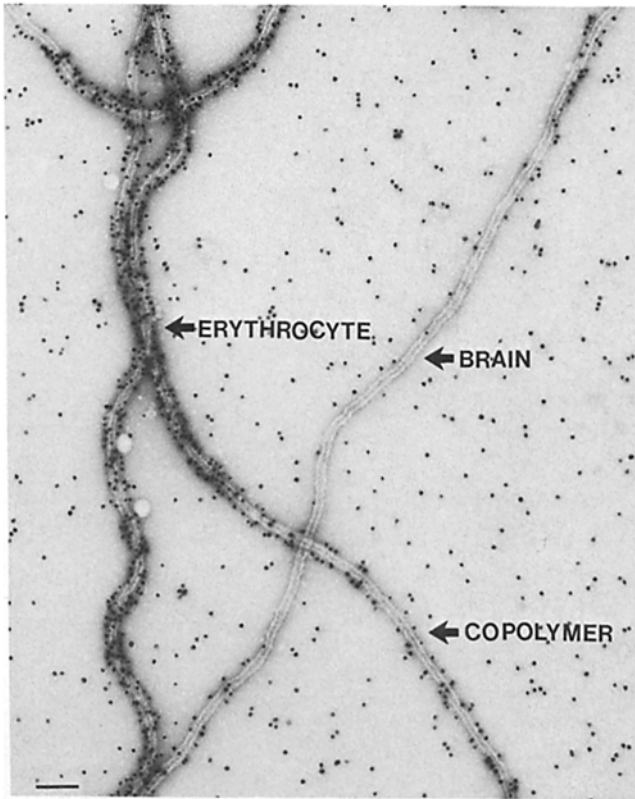


Figure 4. Demonstration of erythrocyte, brain, and mixed tubulin domains within annealed heteropolymers. Annealed microtubules, labeled with erythrocyte β -tubulin antibody and protein A-gold, display levels of gold density which allow identification of erythrocyte, brain, or mixed tubulin copolymers. Bar, 0.1 μ m.

Demonstration of Three Distinct Domains in Annealed Heteropolymers

The primary objective of this study was to evaluate the relative contributions of polymer annealing and subunit exchange to microtubule dynamics at steady state. To examine the mechanisms associated with this process, we used an immunogold-labeling procedure and a rabbit antiserum specific for the β -subunit of erythrocyte tubulin to distinguish three different polymer types. As shown in Figs. 4 and 5, these included the following patterns and corresponding densities of labeling: (a) unlabeled brain tubulin polymer (8 ± 6 gold particles/ μ m), (b) heavily labeled erythrocyte polymer (128 ± 22 gold particles/ μ m), and (c) copolymers composed of a mixture of brain and erythrocyte tubulin subunits with an intermediate level of labeling (76 ± 12 gold particles/ μ m). From studies of microtubule elongation, we determined that copolymers composed of a mixture of tubulin subunits arise at steady state and that the rate of copolymer formation is limited by the rate at which subunits become available from the depolymerization of preexisting erythrocyte and brain microtubules. We used the immunogold labeling procedure to monitor changes in the number and length of preexisting brain and erythrocyte microtubules and of newly formed copolymers. From these observations we calculated the relative contributions of end-to-end joining of preformed microtubules (polymer annealing) and subunit association and dissociation events at microtubule ends (subunit exchange) to microtubule dynamics at steady state.

Table I. Microtubule Annealing under Different Assembly Conditions

Experimental conditions*	Microtubule length [‡]	Concn of MT ends (Molarity $\times 10^6$)	Extent of annealing	Time	Initial rate of
			(% microtubules annealed at $t = x$) [§]		annealing (% microtubules annealed per min)
	μ m		%	min	%
Rothwell, et al., this report					
a. E + B microtubules, sheared	1.9	4.5	57	1	57
b. E + B microtubules, not sheared	5.5	2.8	1	1	1
c. T + D microtubules, no taxol	1.6	1.7	20	10	2
d. T + D microtubules, taxol	1.3	4.3	2	1	2.3
Rothwell et al., 1986a (39)					
e. E + B microtubules, no taxol	1.5	8.3	21	1	21
f. E + B microtubules, taxol	6.6	1.6	15	30	0.5
Kristofferson et al., 1986 (20)					
g. Biotinylated tubulin at microtubule ends	32.0	0.063	6.4	0	—
h. Biotinylated tubulin as seeds	35.8	0.007	2.5	11	0.2
i. Glycerol	14.0	0.068	6.4	0 h	—
Caplow et al., 1986 (4)					
j. B microtubules + axonemes	0.76	0.069	69	10	—

* Rothwell et al. (this report) and Rothwell et al. (39) employed MAP-free chicken brain and erythrocyte tubulin at 5–8 mg/ml that was polymerized in assembly buffer containing 100 mM Na-Pipes at pH 6.94, 1 mM Mg-GTP, and 5% glycerol. Kristofferson et al. (20) used purified, MAP-free bovine brain tubulin to prepare biotinylated or control (untreated) microtubules at 1–2 mg/ml in assembly buffer containing 80 mM Na-Pipes, at pH 6.8, supplemented with 1 mM each EGTA, MgCl₂, and GTP. Caplow et al. (4) used purified pig brain tubulin in pH 6.8 assembly buffer containing 100 mM Na-MES, 6.5 mM MgCl₂, 3.4 M glycerol, 1.0 mM EGTA, 1 mM acetylphosphate, and acetate kinase (0.0750 U/ml). Annealing was documented between pig brain microtubules and *Tetrahymena* axonemes. Notes on experimental conditions: (a) erythrocyte (E) and brain (B) microtubules sheared immediately before mixing; (b) E and B microtubules sheared 10 min prior to mixing; (c) tyrosinolated (T) and detyrosinolated (D) microtubules sheared before mixing; (d) T and D microtubules in 10 μ M taxol, sheared before mixing; (e) E and B microtubules sheared 2 min before mixing; (f) E and B microtubules in 10 μ M taxol, sheared before mixing; (g) unlabeled microtubules elongated in biotinylated tubulin; (h) biotinylated microtubules elongated in unlabeled tubulin; (i) unlabeled microtubules elongated in biotinylated tubulin in glycerol assembly buffer; (j) hog brain microtubules and axonemes in glycerol assembly buffer.

[‡] Microtubule length indicates the mean length of both microtubule types.

[§] Percentage of microtubules annealed = (number of microtubules scored as annealed)/(total number of microtubules) $\times 100$.

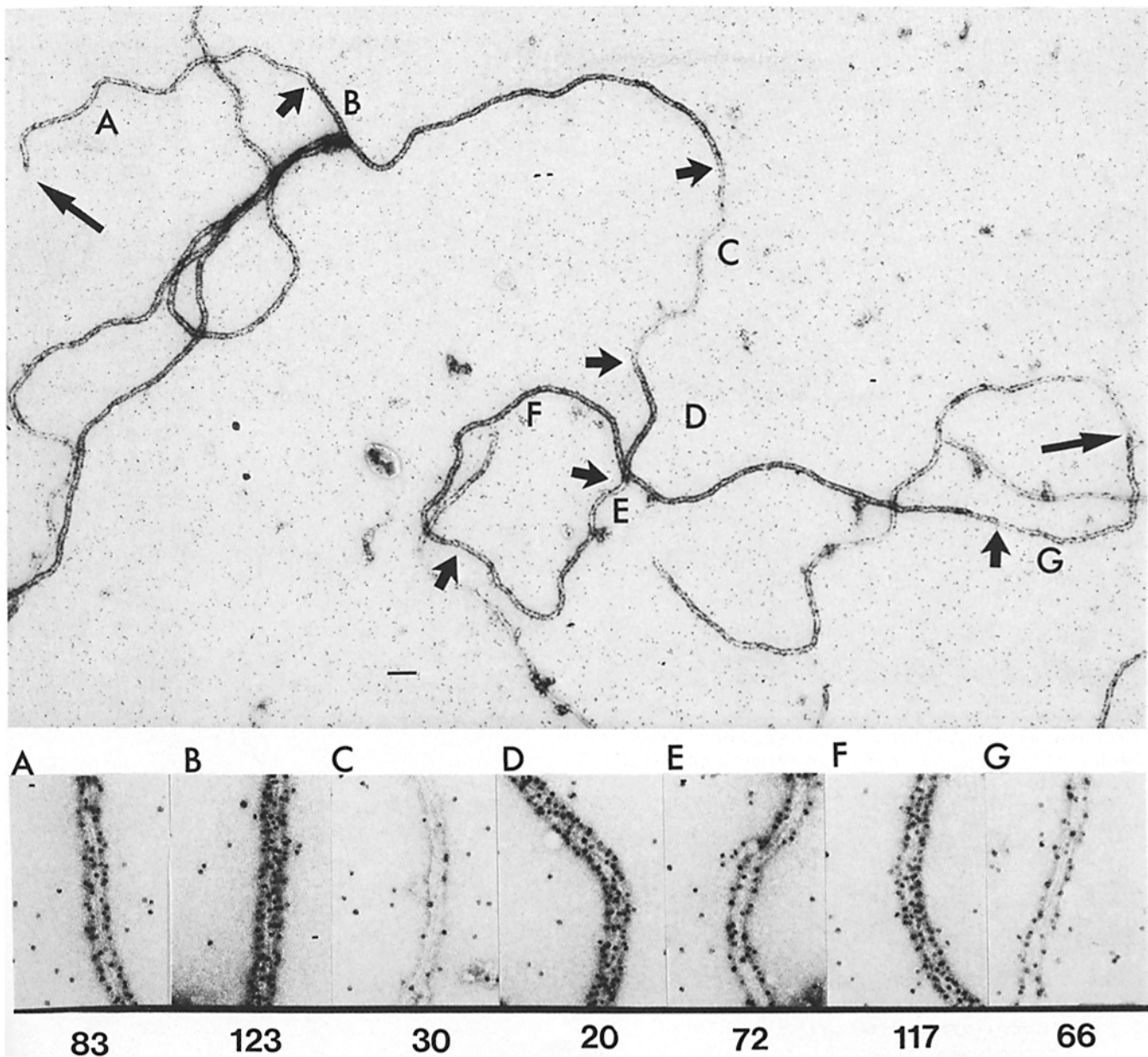


Figure 5. Examination of gold particle density on a heteropolymer with erythrocyte, brain, and copolymer domains. Preformed microtubules polymerized from chicken erythrocyte or brain tubulin were mixed and incubated for 60 min at 37°C before fixation and preparation for immunoelectron microscopy using the erythrocyte beta tubulin antibody and protein A-gold. The bottom panels show high magnification views and the corresponding gold particle density (particles per micrometer) of the regions lettered on the overview. The long arrows mark the ends of the microtubule and the short arrows indicate the boundaries of adjacent domains. Bar, 0.15 μm .

Changes in the Patterns of Microtubule Labeling and Composition



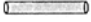
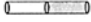


Erythrocyte and brain microtubules were mixed together and examined with respect to changes that occurred in their length, number, and composition. In that we suspected that shearing might alter the rate of annealing or subunit exchange, we conducted parallel experiments in which microtubules were mixed immediately after shearing (case A) or allowed to recover for 10 min after shearing before mixing (case B). These two variables are indicated in Table II and in Figs. 6 and 8.

As shown in Figs. 6 and 7 and summarized in Table II, six different classes of microtubules were observed: (a) microtu-

bules composed entirely of brain tubulin, (b) microtubules composed entirely of erythrocyte tubulin, (c) copolymers composed of a mixture of erythrocyte and brain tubulin, (d) elongated brain microtubules with copolymers on their ends, (e) elongated erythrocyte microtubules with copolymers on their ends, and (f) annealed microtubules composed of variable numbers of distinct tubulin domains. Microtubules were scored as "annealed" only if the pattern could not be attributed to elongation through subunit addition on the ends of preexisting erythrocyte and brain microtubules. This analysis yielded an estimate of the minimum number of annealing events.

Figs. 6 and 7 show the development of complex patterns

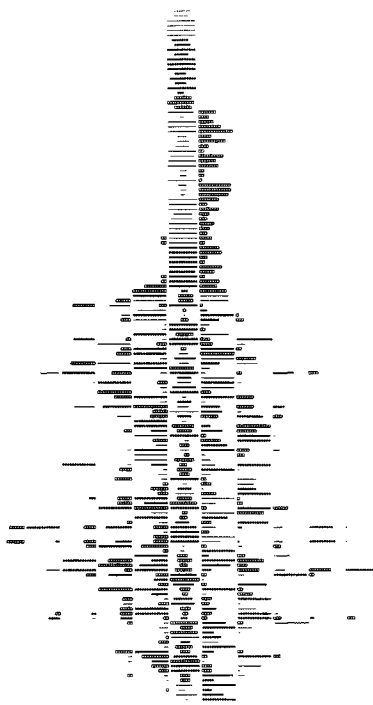
Table II. Changes in the Patterns of Microtubule Composition at Steady State

Microtubule type		Percentage			
		Case A		Case B	
		0 min	60 min	0 min	60 min
Brain		5	0	48	9
Erythrocyte		8	5	41	12
Copolymer		2	4	0	8
Brain-copolymer		19	0	1	11
Eryth-copolymer		6	7	9	16
Annealed		57	77	1	44

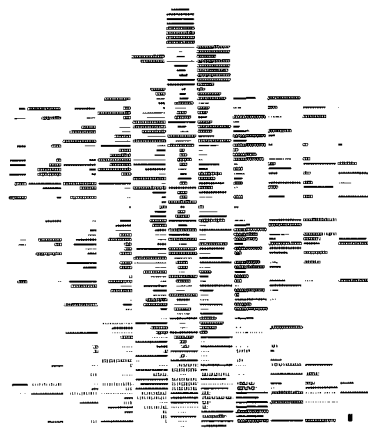
The microtubules shown in Fig. 6 were scored as belonging to one of the six morphologic classes shown in the table. The frequency of each class observed under two different experimental conditions (cases A and B) is indicated.

of annealed microtubules from the simple erythrocyte and brain microtubules present at the time of mixing. It was quite evident that cases *A* and *B*, which differed experimentally only in the time allowed between shearing and mixing the samples, displayed great differences in the rate and extent of annealing. In case *A*, where the microtubules were mixed immediately after shearing, the rate of annealing was so great that 57% of the microtubules were annealed at 10 s (the time required to take the first sample). As seen in a detailed view of case *A* at $t = 10$ s (Fig. 7), the dynamics of microtubule behavior within the first few seconds were rapid and complex. Significant numbers of new copolymers formed, which were observed as elongated segments on the ends of original polymers and as distinct domains within annealed heteropolymers. By 60 min the proportion of annealed microtubules increased to 77% of the sample. If microtubules were

A

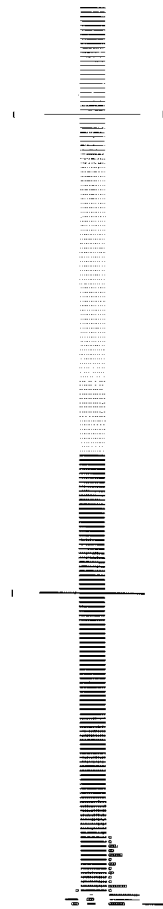


0 min

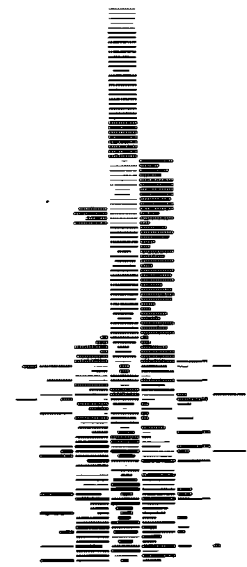


60 min

B



0 min



60 min

Figure 6. Overview of microtubule dynamics in vitro. The figure shows the transition from simple to complex combinations of domains within individual microtubules for two experimental conditions (cases *A* and *B*) and at two different times (0 and 60 min). The lengths of brain (— — —), erythrocyte (●●●), and copolymer (□□□) segments were measured and plotted as segmented horizontal lines, with each set of lines representing a single microtubule. Domains have been truncated for clarity, with the width of each column representing a length of 0.9 μm . Although this figure understates the variability of domain length, the overall pattern of polymer annealing is emphasized. For case *b*, 10 s, the mean and standard deviation for the length of brain and erythrocyte tubulin domains are 3.47 ± 1.90 and 3.61 ± 1.84 μm , respectively. Details regarding the numbers and lengths of domains and the frequency of occurrence of different patterns of arrangement are presented in Fig. 8 and in Table II.

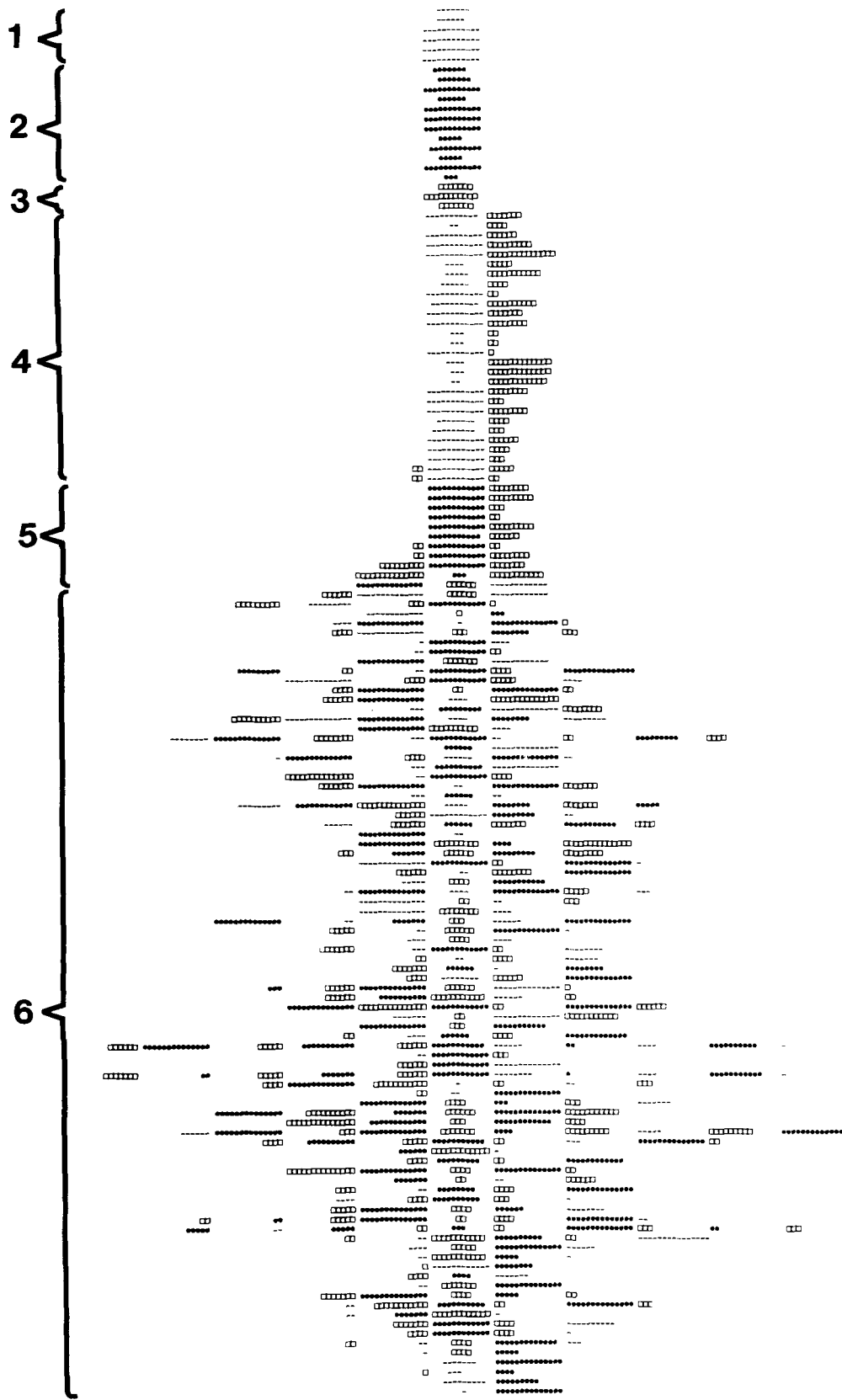


Figure 7. A detailed graphic representation of microtubules sampled at 0 min in case A ([- - -] brain tubulin domains; [●●●] erythrocyte tubulin domains; [□□□] copolymer domains). Microtubules are grouped in the following classes: 1. brain tubulin microtubules, 2. erythrocyte tubulin microtubules, 3. copolymers formed from brain and erythrocyte tubulin, 4. brain tubulin microtubules with copolymer elongation, 5. erythrocyte tubulin microtubules with copolymer elongation, and 6. annealed microtubules.

allowed to recover 10 min before mixing (case B), both the initial rate and the extent of annealing were substantially reduced; only 1% of the microtubules were annealed at 10 s, with most of the microtubules being represented by either

erythrocyte or brain microtubules (89%). After 60 min, however, the proportion of annealed microtubules increased to 44% and the numbers of preexisting brain and erythrocyte microtubules declined. Thus, in these preparations contain-

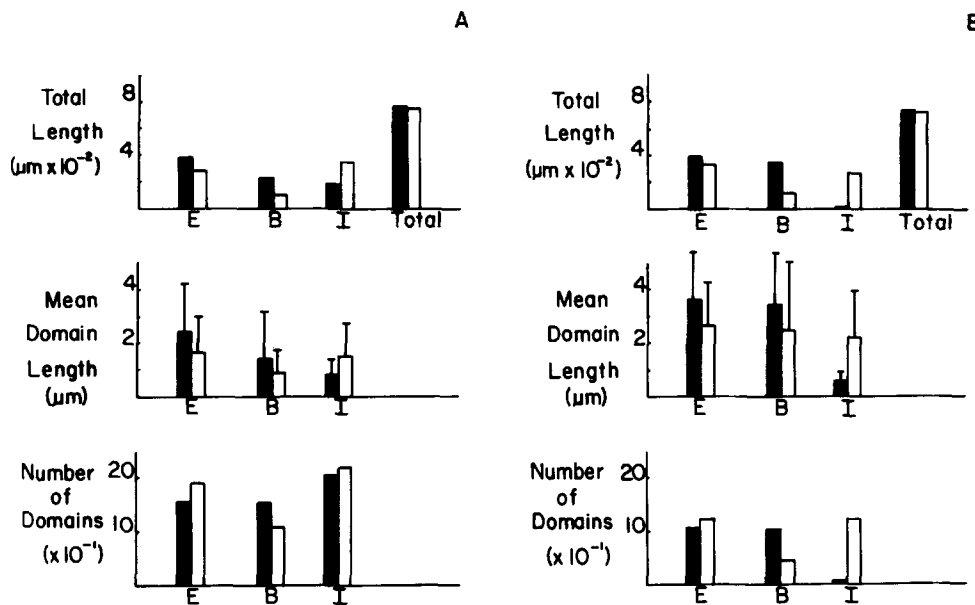


Figure 8. Changes in the size and number of microtubule domains. Microtubules from each sample shown in Fig. 6 ($\sim 750 \mu\text{m}$ in total length) were analyzed by measuring total domain length as well as the mean domain length and number. The figure shows data for two experimental conditions (cases *A* and *B*) and at two different times (10 s, solid bars; and 60 min, open bars). The three classes of microtubules are defined in terms of the density of labeling as erythrocyte (*E*), brain (*B*), and intermediate (*I*). The last category indicates copolymers composed of a mixture of brain and erythrocyte tubulin subunits. Total length and microtubule number for each experimental condition were as follows: case *A* 0 min: $768 \mu\text{m}$, $n = 150$; (2) case *A*, 60 min: $742 \mu\text{m}$, $n = 91$; (3) case *B* 0 min: $750 \mu\text{m}$, $n = 206$; (4) case *B*, 60 min: $740 \mu\text{m}$, $n = 120$. Error bars represent the standard deviation of the domain length.

ing erythrocyte microtubules and brain microtubules, annealing was observed to be an important component of microtubule dynamics in vitro, and appeared to be potentiated by shearing.

Changes in the Length and Number of Microtubule Domains

To evaluate the relative contributions of polymer annealing and subunit exchange to microtubule dynamics, we first determined the lengths and numbers of all microtubule domains contained in $750 \mu\text{m}$ of total polymer length. Data are shown for microtubules sampled at 10 s (solid bars) and 60 min (open bars) after mixing (Fig. 8). Conditions *A* and *B* represent experiments in which microtubules were mixed immediately after shearing (*A*) or allowed to recover for 10 min after shearing before mixing (*B*). In that microtubule number decreased with time, we measured a total of $750 \mu\text{m}$ of total polymer length for each time point (10 s and 60 min) and condition (*A*, *B*) rather than a specified number of polymers. For each sample we determined total length (sum of the lengths of all domains for each tubulin type), the number of domains, and the mean domain length. In both case *A* and case *B*, microtubule number declined and the mean microtubule length increased as follows: (a) For case *A*, the number fell from 150 to 91 (40% decrease) in 60 min, while the mean length increased from 5.1 to $7.9 \mu\text{m}$ (57% increase). (b) For case *B*, the number declined from 206 to 120 (42% decrease) after 60 min, while the mean length increased from 3.6 to $6.2 \mu\text{m}$ (72% increase).

Fig. 8 shows that for cases *A* and *B*: (a) the total length of the erythrocyte tubulin domains (*E*) and brain tubulin do-

main (*B*) declined between 10 s and 60 min (Fig. 8, top panel) while the total length of copolymers with intermediate labeling (*I*) increased. Further, the amount of depolymerization (defined as the loss of original erythrocyte and brain polymer) was balanced by an equal amount of assembly of copolymer (29% depolymerization vs. 22% copolymer assembly for case *A*, and 39% depolymerization vs. 37% copolymer assembly for case *B*). The near equivalence in the gain and loss of polymer types indicates that the samples were close to polymer mass steady state. This was particularly evident in case *B*. In the absence of steady-state conditions, one would have predicted a greater amount of copolymer formation than depolymerization of preexisting microtubules, but this was not observed. (b) The mean lengths of the erythrocyte and brain tubulin domains declined by ~ 23 – 35% (Fig. 8, middle panel). (c) The number of erythrocyte and brain tubulin domains remained the same or decreased slightly with time (Fig. 8, bottom panel). Of the two tubulin types, brain microtubules appeared to be more unstable. Thus, a large loss in the number of original erythrocyte and brain microtubules through depolymerization did not occur.

Relative Contributions of Polymer Annealing and Subunit Exchange to Microtubule Dynamics

We calculated the relative contributions of polymer annealing and subunit exchange to microtubule dynamics based on our ability to distinguish annealed from nonannealed microtubules and microtubules that contained newly elongated copolymer. We estimated the contributions of annealing by counting the numbers of joining sites contained within

Table III. Relative Contributions of Polymer Annealing and Subunit Exchange to Microtubule Dynamics at Steady State*

Parameter	Length and number		Change in length and number	Change due to annealing	Change due to subunit exchange
	$t = 0$	$t = 60$ min			
Mean length (μm)	3.6	6.2	2.6	2.0 [‡] (77%)	0.6 [§] (23%)
Number	206	120	86	56 (58%)	40 [†] (42%)

* The relative contributions of polymer annealing and subunit exchange to the redistribution of microtubule length and number were calculated from the lengths and numbers of microtubules in an experiment in which samples of brain and erythrocyte microtubules at 5 mg/ml were sheared and allowed to recover to steady state before mixing (case B in Fig. 6). The mixture was examined 10 s after mixing ($t = 0$) and after 1 h ($t = 60$ min). For each time point a total length of 750 μm polymer was analyzed.

[‡] Change in length due to polymer annealing was calculated as the difference in the mean lengths at $t = 60$ min of microtubules in the entire sample (6.2 μm) and of the nonannealed microtubules (4.2 μm). At $t = 60$ min, many microtubules have undergone annealing, resulting in polymers with considerably longer lengths. As a result, the mean length of the microtubules that have not annealed is less than that of the population as a whole, and the difference in their mean lengths represents the change due to polymer annealing.

[§] Increase in microtubule length due to mechanisms of subunit exchange was calculated as the difference in the lengths of nonannealed at $t = 60$ min (4.2 μm) and at $t = 0$ (3.6 μm).

^{||} Decrease in microtubule number due to polymer annealing was determined by analyzing the microtubules and counting the minimum number of annealing events required to give the observed patterns at $t = 60$ min (56 events). The actual number of annealing events is probably somewhat higher due to homologous microtubule annealing events that cannot be observed.

[†] Decrease in microtubule number due to subunit exchange was calculated as the difference in the total number of erythrocyte and brain tubulin segments present in the sample at $t = 0$ (210 domains) and at $t = 60$ min (170 domains). Because each erythrocyte and brain tubulin domain observed at $t = 60$ min represents one of the original microtubules present at $t = 0$, a decrease in the number of domains is a direct measure of the number of microtubules lost by depolymerization. As seen in Fig. 8, the appearance of copolymer at $t = 60$ min can best be accounted for by an overall shortening of the original erythrocyte and brain microtubules, rather than by the depolymerization of large numbers of preexisting microtubules. The number of erythrocyte tubulin domains remained essentially unchanged, whereas the number of brain tubulin domains decreased by about half, representing a 25% decrease in the number of original domains.

annealed heteropolymers and by analyzing heteropolymer lengths. In a similar fashion, we estimated the effects of subunit exchange on microtubule dynamics by analyzing the lengths of copolymer domains. Inasmuch as the populations we examined were at or close to polymer mass steady state, we assumed that the length of copolymers directly indicated the extent of disassembly of preexisting brain and erythrocyte microtubules.

An analysis of the dynamics exhibited by the microtubules in case B, shown previously in Figs. 6 and 8, is presented in Table III. As described above in the previous section, there was good evidence that the microtubules contained in this sample were at steady state before the time of mixing. After 60 min the mean length of the microtubules increased by 2.6 μm , of which 2.0 μm (77%) was estimated to be due to annealing and 0.6 μm (23%) was due to subunit exchange. Under these conditions, annealing appeared to be a major cause for the increase in polymer length. In contrast, both annealing and subunit exchange (a process dependent on microtubule disassembly) contributed significantly to the reduction in microtubule number (58% due to annealing and 42% to subunit exchange).

We consider these calculations to be only an estimation of the relative contributions of annealing and subunit exchange to microtubule dynamics. At the present time, ambiguities in the exact histories of individual polymers and lack of information regarding the mechanism of annealing prevent a precise analytic description of the events involved. For example, one area of uncertainty is the determination of the number of annealing events. Because we could not identify homologous annealing events or estimate this number with any degree of accuracy, we chose to use for our calculation only the minimum number of events we could deduce had occurred between heterologous polymers even though this resulted in an underestimation of the true number of annealing events. However, we believe that the present method, which is based on changes in the average lengths and numbers of

polymers, adequately describes the overall dynamics. As a final check on the validity of this method for approximating the relative contributions of these dynamic processes, we point out that the estimates for changes in polymer length, although calculated separately, add up to give the change that was actually observed. The estimated decreases in microtubule number do not precisely add up to the actual observed value, probably due to a certain degree of ambiguity in determining the number of annealing events.

Owing to the rapid and complex dynamics exhibited by the microtubules in case A, it has so far not been possible to analyze the dynamics of this sample with the same degree of confidence. However, by applying certain corrections we observed that the contributions of polymer annealing and subunit exchange were similar to those observed in case B. A precise description of the events that occurred under these conditions must await future analysis.

Discussion

Annealing Is a General Property of Cytoplasmic Microtubules

Because the assembly properties of erythrocyte tubulin differ significantly from those of brain tubulin (31, 32), we were interested in determining whether annealing was a unique property of erythrocyte tubulin. In the present paper we report that brain microtubules also anneal efficiently with each other, indicating that annealing may be a general property of all cytoplasmic microtubules. Although homologous brain microtubules annealed, the initial rate of annealing (2%/min) was determined to be 10–20-fold smaller than the initial rate of annealing between erythrocyte and brain microtubules (21–57%/min, Table I). The reason for the greater rates of annealing associated with erythrocyte microtubules is not yet understood. One possibility is that annealing is sensitive to experimental conditions such as polymer concentration

and length. Another possible explanation is that the greater rate of annealing of erythrocyte microtubules reflects the larger association and dissociation rate constants of erythrocyte tubulin; however, the relationships between polymer annealing and subunit exchange have not yet been determined. (For further discussion, see below.)

Effects of Shearing on Microtubule Annealing

We observed that shearing caused a temporary increase in the rate of annealing and had a large effect on the overall dynamics of the microtubules (Fig. 6). Furthermore, although the concentrations of microtubule ends differed by a factor of only two in cases *A* and *B* (calculated from Fig. 7, *middle panel*), the initial rate of annealing increased 57-fold. It is clear that the rapid reduction in microtubule numbers after shearing was not due to the complete depolymerization of large numbers of microtubules. Rather, the majority of microtubules persisted, and shearing appeared instead to enhance the rate of polymer annealing.

The explanation for how shearing increased the rate of annealing is not yet understood, although several mechanisms may be considered. (a) Shearing may enhance the rate of annealing by decreasing the microtubule length and/or by increasing the concentration of microtubule ends. (b) Shearing may physically alter the structure or composition of the microtubule ends. The ends may become frayed, thereby increasing the probability of successful end-to-end interactions. Alternatively, broken microtubules ending in GDP-tubulin subunits may anneal more efficiently than intact microtubules ending in GTP-tubulin caps. However, preliminary studies on actin filament annealing reveal that preparations containing ATP-actin anneal at approximately the same rate as do preparations containing only ADP-actin (Murphy et al., manuscript in preparation). (c) Shearing may transiently depolymerize microtubules and increase the tubulin subunit concentration, a condition which may facilitate annealing. Preparations that were mixed immediately after shearing revealed extensive copolymer formation. In that conditions that decrease the tubulin subunit concentration such as assembly in the presence of taxol have been observed to decrease the annealing rate (39), we feel that the increased rate of annealing induced by shearing could be associated with a temporary increase in subunit exchange activity.

Effects of Microtubule Length and Number Concentration on Annealing

For a bimolecular reaction involving the collision of two polymer ends, the rate of annealing should be proportional to the square of the concentration of the ends. Hence, a 100-fold increase in the concentration of ends should give rise to a 10,000-fold increase in the annealing rate. To test this prediction, we examined microtubule annealing rates over a 150-fold range of concentrations of microtubule ends under conditions where polymer lengths and the ratio of erythrocyte and brain polymers remained constant (the total protein concentration in these experiments ranged 0.1–15.3 mg/ml). However, no consistent dependence of the rate of annealing on the concentration of polymer ends was observed (data not shown).

We also examined the effect of polymer length on polymer annealing, inasmuch as longer polymers are predicted to

have smaller diffusion coefficients and exhibit lower rates of annealing (12). However, we detected no consistent relationship between polymer length and annealing rates for microtubules whose lengths varied by a factor of 2–5. Over a considerable range of lengths and concentrations the annealing rates remained similar. These results agree with a previous report on microtubule annealing in which we also observed that annealing was not a diffusion-limited process (39). We propose several reasons why microtubule annealing does not appear to obey second-order kinetics:

(a) Microtubule annealing *in vitro* may be limited by the tendency of long-length polymers to become oriented into parallel bundles by microscopic flow in the preparation. Observation of native microtubules by darkfield microscopy indicates that microtubules rapidly become organized into bundles due to fluid flow, even after shearing to relatively short, 1- μ m lengths. The alignment of polymers has been shown to account for the opalescence and flow birefringence of microtubules and actin filaments in solution. The ordering effects of flow would be expected to greatly reduce the ability of long-length polymers to freely diffuse in solution. In light of these considerations, it may, therefore, be useful to examine rates of annealing under conditions that allow free diffusion of polymers.

(b) Comparison of the rates of annealing in cases *A* and *B* suggests that microtubule populations may exhibit biphasic annealing kinetics. When freshly sheared microtubules were analyzed, we discovered that the bulk of the annealing occurred within the first several seconds. This rapid phase of annealing which lasted for a few seconds was followed by a slower phase which lasted several hours. When the erythrocyte and brain microtubules were allowed to return to an unperturbed state before mixing, only the slow phase of annealing was observed. A similar pattern of rapid and slow phases of annealing has also been reported for actin filaments (Murphy et al., manuscript in preparation). These results suggest that the determination of annealing rate constants may require sampling on a much shorter time scale than was previously envisioned.

The Contribution of Annealing to Microtubule Dynamics

This study establishes that annealing contributes significantly to the dynamics of microtubules *in vitro*. When microtubules are mixed under steady-state conditions, polymer annealing accounts for much of the increase in the microtubule length at steady state. Although the mechanism is not yet completely understood, it appears that polymer annealing may be related to and dependent on mechanisms of subunit exchange at the ends of microtubules. Recently, Kristofferson et al. (20) described the dynamics of microtubule behavior after mixing together untreated and biotinylated microtubule polymers. At steady state, the microtubules in their experiments became fewer in number and longer in length, a phenomenon which Mitchison and Kirschner have termed dynamic instability (29). They subsequently demonstrated similar behavior for microtubules *in vivo* (27, 42). However, our interpretations of the mechanisms of microtubule dynamics differ significantly from those of Kristofferson and co-workers (20). Although both of our laboratories used similar preparations of microtubules and observed a reduc-

tion in microtubule number and an increase in microtubule length, we attribute much of the decline in number to both annealing and subunit exchange, whereas Kristofferson et al. consider dynamic instability to be due to mechanisms of subunit exchange alone. A comparison of the conditions and results of our experiments is presented in Table I. It is possible that the differences in the rate and extent of annealing reflect differences in experimental conditions and the kinds of microtubule preparations used in the experiments (such as the absence or presence of glycerol and the length and concentration of polymers). Clearly, the details of annealing are not yet understood, and the roles of tubulin subunits and accessory factors such as MAPs and GTP remain to be determined.

Although annealing *in vivo* has yet to be demonstrated, there are many examples where annealing could be functionally significant in generating microtubule organelles and repairing broken microtubules in living cells, particularly in regions containing large numbers of aligned microtubules. For example, annealing may be responsible for generating the long microtubules contained in the marginal bands of platelets and other nucleated blood cells (2). In some cases the microtubule bundle in blood cells is thought to consist of a coiled hoop of just a single microtubule (10, 33). Annealing may also be important for the repair of breaks in microtubule bundles such as those in the processes of neuronal cells (41, 46). In addition, annealing may also be involved in the dynamics and growth of fibers in the mitotic spindle (24–26, 35, 44) or the phragmoplasts in dividing plant cells (16, 17, 23). Finally, it is interesting to speculate whether annealing may be associated with specific microtubule-capturing events, such as the attachment of kinetochores to the ends of exogenous microtubules, as was recently demonstrated *in vitro* by Mitchison and Kirschner (30). Clearly, further work will be necessary to establish the possible contribution of annealing to the dynamic activities of microtubules in the cell.

We thank Dr. Thomas Pollard for the gift of tyrosinolated tubulin antibody and Dr. Edward Salmon for stimulating discussions on the topic of polymer annealing. We also thank Dover Poultry Products Company (Baltimore, MD) for allowing us to collect materials for the isolation of tubulin.

This work was supported by National Institutes of Health grant GM-33171.

Received for publication 5 May 1986, and in revised form 25 February 1987.

References

- Barra, H. S., C. A. Arce, J. A. Rodriguez, and R. Caputto. 1973. Incorporation of phenylalanine as a single unit into rat brain protein: reciprocal inhibition by phenylalanine and tyrosine of their respective incorporations. *J. Neurochem.* 21:1241–1251.
- Behnke, O. 1970. Microtubules in disk-shaped blood cells. *Int. Rev. Pathol.* 9:1–92.
- Bradford, M. 1976. A rapid and sensitive method for the quantitation of microgram quantities of protein utilizing the principle of protein-dye binding. *Anal. Biochem.* 72:248–254.
- Caplow, M., J. Shanks, and B. P. Brylawski. 1986. Differentiation between dynamic instability and end-to-end annealing models for length changes of steady-state microtubules. *J. Biol. Chem.* 261:16233–16240.
- Carlier, M.-F. 1982. Guanosine-5'-triphosphate hydrolysis and tubulin polymerization. *Mol. Cell. Biochem.* 47:97–113.
- Carlier, M.-F., T. L. Hill, and Y. Chen. 1984. Interference of GTP hydrolysis in the mechanism of microtubule assembly: an experimental study. *Proc. Natl. Acad. Sci. USA.* 81:771–775.
- Carlier, M.-F., and D. Pantaloni. 1982. Assembly of microtubule protein: role of guanosine di- and triphosphate nucleotides. *Biochemistry.* 21:1215–1224.
- Carlier, M., and D. Pantaloni. 1983. Taxol effect on tubulin polymerization and associated guanosine 5' triphosphate hydrolysis. *Biochemistry.* 22:4814–4822.
- Dentler, W. L., S. Granett, and J. L. Rosenbaum. 1975. Ultrastructural localization of the high molecular weight proteins with *in vitro*-assembled brain microtubules. *J. Cell Biol.* 65:237–241.
- Euteneur, U., H. Ris, and G. G. Borisy. 1985. Polarity of marginal band microtubules in vertebrate erythrocytes. *Eur. J. Cell Biol.* 39:149–155.
- Felber, J. P., T. L. Coombs, and B. L. Vallee. 1962. The mechanism of inhibition of carboxypeptidase A by 1,10-phenanthroline. *Biochemistry.* 1:231–238.
- Hill, T. L. 1983. Length dependence of rate constants for end-to-end association and dissociation of equilibrium linear aggregates. *Biophys. J.* 44:285–288.
- Hill, T. L. 1984. Introductory analysis of the GTP-cap phase-change kinetics at the end of a microtubule. *Proc. Natl. Acad. Sci. USA.* 81:6728–6732.
- Hill, T. L., and M.-F. Carlier. 1983. Steady state theory of the interference of GTP hydrolysis in the mechanism of microtubule assembly. *Proc. Natl. Acad. Sci. USA.* 80:7234–7238.
- Hill, T. L., and Y. Chen. 1984. Phase changes at the end of a microtubule with GTP cap. *Proc. Natl. Acad. Sci. USA.* 81:5772–5778.
- Jensen, C. G. 1982. Dynamics of spindle microtubule organization: kinetochore fiber microtubules of plant endosperm. *J. Cell Biol.* 92:540–558.
- Jensen, C., and A. Bajer. 1973. Spindle dynamics and arrangements of microtubules. *Chromosoma (Berl.).* 94:73–89.
- Johnson, K. A., and G. G. Borisy. 1977. Kinetic analysis of microtubule self-assembly *in vitro*. *J. Mol. Biol.* 117:1–31.
- Kilmartin, J. V., B. Wright, and C. Milstein. 1982. Rat monoclonal anti-tubulin antibodies derived by using a new nonsecreting rat cell line. *J. Cell Biol.* 93:576–582.
- Kristofferson, D., T. Mitchison, and M. Kirschner. 1986. Direct observation of steady-state microtubules dynamics. *J. Cell Biol.* 102:1007–1019.
- Kristofferson, D., and D. L. Purich. 1981. Time scale of microtubule length redistribution. *Arch. Biochem. Biophys.* 211:222–226.
- Kumar, N., and M. Flavin. 1982. Modulation of some parameters of assembly of microtubules *in vitro* by tyrosinolation of tubulin. *Eur. J. Biochem.* 128:215–223.
- Lambert, A.-M., and A. Bajer. 1972. Dynamics of spindle fibers and microtubules during anaphase and phragmoplast formation. *Chromosoma (Berl.).* 39:101–144.
- McIntosh, J. R., W. Z. Cande, and J. A. Snyder. 1975. Structure and physiology of the mammalian mitotic spindle. In *Molecules and Cell Movement*. S. Inoue and R. E. Stephens, eds. Raven Press, New York. 31–75.
- McIntosh, J. R., and S. Landis. 1971. The distribution of spindle microtubules during mitosis in cultured human cells. *J. Cell Biol.* 49:468–497.
- McIntosh, J. R., K. L. McDonald, M. K. Edwards, and B. M. Ross. Three dimensional structure of the central mitotic spindle of *Diatoma vulgare*. *J. Cell Biol.* 83:428–442.
- Mitchison, T., L. Evans, E. Schultz, and M. Kirschner. 1986. Sites of microtubule assembly and disassembly in the mitotic spindle. *Cell.* 45:515–527.
- Mitchison, T., and M. Kirschner. 1984. Microtubule assembly nucleated by isolated centrosomes. *Nature (Lond.).* 312:232–237.
- Mitchison, T., and M. Kirschner. 1984. Dynamic instability of microtubule growth. *Nature (Lond.).* 312:237–242.
- Mitchison, T., and M. W. Kirschner. 1985. Properties of the kinetochore *in vitro*. II. Microtubule capture and ATP-dependent translocation. *J. Cell Biol.* 101:766–777.
- Murphy, D. B., and K. T. Wallis. 1983. Brain and erythrocyte microtubules from chicken contain different beta-tubulin polypeptides. *J. Biol. Chem.* 258:7870–7885.
- Murphy, D. B., and K. T. Wallis. 1983. Isolation of microtubule protein from chicken erythrocytes and determination of the critical concentration for tubulin polymerization *in vitro* and *in vivo*. *J. Biol. Chem.* 258:8357–8364.
- Nachmias, V. T. 1980. Cytoskeleton of human platelets at rest and after spreading. *J. Cell Biol.* 86:795–802.
- Nath, J., and M. Flavin. 1980. An apparent paradox in the occurrence, and the *in vivo* turnover, of C-terminal tyrosine in membrane-bound tubulin of brain. *J. Neurochem.* 35:693–706.
- Nicklas, R. B., and D. F. Kubai. 1985. Microtubules, chromosome movement and reorientation after chromosomes are detached from the spindle by micromanipulation. *Chromosoma (Berl.).* 92:313–324.
- Raybin, D., and M. Flavin. 1977. Modification of tubulin by tyrosylation in cells and extracts and its effects on assembly *in vitro*. *J. Cell Biol.* 73:492–504.
- Roobol, A., C. I. Pogson, and K. Gull. 1980. Identification and characterization of microtubule protein from myxamoebae of *Physarum polycephalum*. *Biochem. J.* 198:305–312.
- Rothwell, S. W., W. A. Grasser, and D. B. Murphy. 1985. Direct observation of microtubule treadmilling by electron microscopy. *J. Cell Biol.* 101:1–6.
- Rothwell, S. W., W. A. Grasser, and D. B. Murphy. 1986a. End-to-end annealing of microtubules *in vitro*. *J. Cell Biol.* 102:619–627.

40. Rothwell, S. W., W. A. Grasser, and D. B. Murphy. 1986b. Tubulin variants exhibit different assembly properties. *Ann. N.Y. Acad. Sci.* 466: 103-110.
41. Schliwa, M. 1984. Mechanisms of intracellular transport. *Cell Muscle Motil.* 5:1-81.
42. Schultz, E., and M. Kirschner. 1986. Microtubule dynamics in interphase cells. *J. Cell Biol.* 102:1020-1031.
43. Slot, J. W., and H. J. Geuze. 1981. Sizing of protein A-colloidal gold probes for immunoelectron microscopy. *J. Cell Biol.* 90:533-535.
44. Tippet, D. H., C. T. Fields, K. L. O'Donnell, J. D. Pickett-Heaps, and D. J. McLaughlin. 1984. The organization of microtubules during anaphase and telophase spindle elongation in the rust fungus *Puccinia*. *Eur. J. Cell Biol.* 34:34-44.
45. Towbin, H., T. Staehlin, and J. Gordon. 1979. Electrophoretic transfer of proteins from polyacrylamide gels to nitrocellulose sheets: procedures and some applications. *Proc. Natl. Acad. Sci. USA.* 76:4350-4354.
46. Wadsworth, P., and E. D. Salmon. 1986. Analysis of the treadmilling model during metaphase of mitosis using fluorescence redistribution after photobleaching. *J. Cell Biol.* 102:1032-1038.
47. Wehland, J., M. C. Willingham, and I. Sandoval. 1983. A rat monoclonal antibody reacting specifically with the tyrosylated form of alpha-tubulin. I. Biochemical characterization, effects of microtubule polymerization and organization in vitro. *J. Cell Biol.* 97:1467-1475.